

# Isothermal Crystallization Kinetics of Commercially Important Polyalkylene Terephthalates

B. J. CHISHOLM,\* J. G. ZIMMER

GE Plastics, One Lexan Lane, Mt. Vernon, Indiana 47620

Received 1 July 1999; accepted 7 October 1999

**ABSTRACT:** The isothermal crystallization kinetics of virgin, melt-mixed, and nucleated specimens of polyethylene terephthalate (PET), polypropylene terephthalate (PPT), and polybutylene terephthalate (PBT) were measured. The purpose of the study was to determine the difference in crystallization rate of PPT, which is to be commercially available in the near future, to the extensively studied, commercially important polyalkylene terephthalates PET and PBT. At equivalent supercooling, the crystallization rate of PPT was between that of PET and PBT, with PBT being the fastest crystallizing polymer. Melt-mixing virgin materials resulted in a substantial increase in the crystallization rate for all three polyalkylene terephthalates. The addition of talc or sodium stearate as a nucleating agent resulted in a further increase in crystallization rate for all three polyesters. Although the addition of talc or sodium stearate to PPT and PET greatly enhanced crystallization rate, these nucleating agent-containing materials still did not crystallize as fast as PBT melt-mixed in the absence of any intentionally added nucleating agents. Analysis of the crystallization kinetic data using the Avrami equation showed that melt-mixing and the addition of sodium stearate resulted in an increase in the average Avrami exponent. This result suggested a change in the mechanism of nucleation toward more sporadic nucleation. For the sodium stearate-nucleated materials, the Avrami exponent was found to increase with increasing crystallization temperature, but a precise explanation of this behavior could not be provided without a knowledge of crystallite morphology. © 2000 John Wiley & Sons, Inc. *J Appl Polym Sci* 76: 1296–1307, 2000

**Key words:** polyester; crystallization kinetics; polybutylene terephthalate; polypropylene terephthalate; polyethylene terephthalate

## INTRODUCTION

Recently, Shell Chemical Company announced its intent to commercialize polypropylene terephthalate (PPT) for both fiber and injection-molding applications.<sup>1</sup> This decision was the result of a new process innovation for the production of 1,3-

propanediol at a much lower cost.<sup>2</sup> The fiber properties of PPT have been the subject of several reports,<sup>3–6</sup> whereas only a few reports describe the properties of injection-molded specimens.<sup>1,7</sup>

A very important characteristic of semicrystalline polymers that strongly influences the utility of the material for a given application is crystallization rate. For example, polyethylene terephthalate (PET), used extensively in fiber and packaging applications, possesses a relatively minor share of the injection-molding market because of its relatively slow rate of crystallization. In contrast, polybutylene terephthalate (PBT) is used extensively for injection-molding applica-

Correspondence to: B. J. Chisholm (chisholm@crd.ge.com).

\* Present address: General Electric Corporate Research and Development, Polymer Materials Laboratory, One Research Circle, Niskayuna, NY 12309.

*Journal of Applied Polymer Science*, Vol. 76, 1296–1307 (2000)  
© 2000 John Wiley & Sons, Inc.

tions because of its relatively fast crystallization rate. Fast crystallization allows for high production rates of molded articles, since the time needed for the material to solidify in the mold is a function of crystallization rate.

Although numerous reports exist describing the crystallization kinetics of PET<sup>8-12</sup> and PBT,<sup>13-16</sup> only the reports by Bulkin and coworkers<sup>17,18</sup> were found describing the crystallization kinetics of PPT. These authors measured the crystallization kinetics of PPT from the glassy state, using vibrational spectroscopy. Considering the importance of crystallization rate to the commercial utility of a thermoplastic polyester, a comparison of the crystallization rates of PPT to PBT and PET was deemed important. The purpose of this report was to compare the crystallization kinetics of PPT to PET and PBT under identical conditions, and to investigate the effect of melt-mixing and the addition of common nucleating agents on crystallization rate.

## EXPERIMENTAL

### Materials

The PET utilized for the investigation was grade D26 from DuPont; PBT and PPT were synthesized by the melt-polymerization of dimethylterephthalate (DMT) and the appropriate diol, using tetraisopropyl titanate (TPT) as catalyst. DMT was obtained from Kosa Corp.; 1,4-butanediol and 1,3-propanediol were obtained from BASF and DeGussa Corp., respectively. Both diols and DMT had a purity of greater than 99%.

A representative polymerization procedure is as follows: 11.7 kg of DMT, 7.35 kg of 1,3-propanediol, and 16.4 mL of TPT were charged to a 10CV Helicone reactor, preheated to 130°C. The monomer mixture was then heated to 225°C at a rate of 1.0°C/min under atmospheric pressure and most of the methanol by-product removed by distillation. The mixture was then subjected to a gradual reduction in pressure to 175 mmHg at a rate of 20 mmHg/min, while the temperature was simultaneously increased to 250°C at a rate of 2.0°C/min. On reaching a pressure of 175 mmHg, the pressure was further reduced to 1.5 mmHg at a rate of 20 mmHg/min and held at that pressure for the remainder of the polymerization. The total time under vacuum was 155 min.

Solid state polymerization (SSP) was used to further build and control the molecular weight of

the samples. SSP was conducted on cylindrical pellets that were approximately 2.0 mm in diameter and 3.0 mm long. The SSP polymerization apparatus was essentially a slowly stirred glass tube with a porous bottom that allowed preheated nitrogen to pass uniformly through the tube. A hot-oil bath was used to heat the reactor and to preheat the nitrogen. The oil temperatures used were 206, 208, and 225°C, respectively, for PBT, PPT, and PET. Reaction progress was monitored by periodically removing 5.0-g samples from the reactor and immediately measuring melt flow index (MFI). On reaching the desired MFI, the remaining material was removed from the reactor and cooled to room temperature under nitrogen.

The talc used was Ultratalc 609 from Barretts Minerals and sodium stearate was obtained from Aldrich Chemical. Both talc and sodium stearate were used at a concentration of 0.50 pph.

### Characterization

Molecular weight was determined using gel permeation chromatography and polystyrene standards. The instrument was a Waters GPC, equipped with an ultraviolet detector set at a wavelength of 254 nm. The column set was Phenogel with pore sizes of 10<sup>5</sup>, 10<sup>4</sup>, and 500 Å. The eluant was chloroform, flowing at a rate of 1.5 mL/minute and the injection size was 10 µL. The samples were made up at an approximate concentration of 2 mg/mL and dissolved in a 10/90 v/v 1,1,1,3,3,3-hexafluoro-2-propanol/chloroform solvent mixture.

MFI was determined at 250°C for PBT-V, 255°C for PPT-V, and 285°C for PET-V, using a Tinius Olsen model UE-4-78 rheometer equipped with a 1200-g weight and 2.083-mm diameter capillary.

Equilibrium melting temperatures and isothermal crystallization kinetics were determined using a Perkin-Elmer DSC7 differential scanning calorimeter. The method for equilibrium melting temperature ( $T_m^c$ ) determination consisted of heating samples from 40°C, at a rate of 20°C/min, to 270°C for PBT, 275°C for PPT, and 305°C for PET, holding at that temperature for 4 min, and then cooling to the crystallization temperature ( $T_c$ ) at a rate of 300°C/min. It was necessary to optimize the time of crystallization for the various polymers and  $T_c$ s so that crystallization ensued without significant annealing of the crystallites. Annealing results in crystallite thickening and, thus, an overrepresentation of the melting tem-

**Table I** Composition of the Polymer Samples Investigated<sup>a</sup>

Sample <sup>b</sup>	MFI (g/10 min)	$M_n$ (g/mol)	$M_w$
PBT-V	20.0	36,600	77,400
PPT-V	21.8	36,300	78,400
PET-V	22.2	32,400	68,400
PBT-M	—	33,000	73,000
PPT-M	—	33,900	70,900
PET-M	—	29,300	61,000
PBT-T	—	32,400	71,500
PPT-T	—	33,200	70,000
PET-T	—	30,100	61,000
PBT-S	—	31,500	69,300
PPT-S	—	29,700	62,300
PET-S	—	25,100	53,000

<sup>a</sup> MFIs of PBT, PPT, and PET samples were measured at 250, 255, and 285°C, respectively.

<sup>b</sup> V and M indicate virgin and melt-mixed samples, respectively; T and S indicate the presence of 0.50 pph talc and sodium stearate, respectively.

perature of the crystallites formed at  $T_c$ .<sup>19</sup> The melting temperature of the crystallites formed at  $T_c$  was determined by subsequently heating the sample from  $T_c$ , using a heating rate of 20°C/min.

Isothermal crystallization kinetics were determined using a modification of the heating and cooling profile used for the determination of  $T_m^o$  described earlier. The modification consisted of an increase in crystallization time to ensure that the entire crystallization isotherm was captured.

All specimens were 3.0–4.0 mg and thoroughly dried before analysis.

### Melt-Mixing

Melt-mixing was accomplished using a Haake mixing bowl operating at a speed of 100 rpm and temperature of 250, 255, and 285°C, respectively, for PBT, PPT, and PET samples. The pellets were dried for 3–4 h at 120°C in a forced-air-circulating oven before melt-mixing. Nucleating agents were added to the dried pellets just before being introduced to the mixing bowl.

## RESULTS AND DISCUSSION

A description of the materials investigated is shown in Table I. This study was designed to compare the isothermal crystallization kinetics of PPT to PBT and PET at equivalent melt viscosity of the virgin polymer samples. MFI was used to

represent the melt viscosity of the polymers, since this measurement is commonly used in the thermoplastics industry.<sup>20</sup> The decision to compare the materials at equivalent melt viscosity, as opposed to equivalent polymer molecular weight, was based on the fact that the melt viscosity of an injection-moldable material generally needs to be tightly controlled for a given application. Nevertheless, the molecular weight of all samples was measured using GPC and reported in Table I.

The recommended injection-molding temperature for commercial PBT-based materials such as GE Plastics' Valox products or Ticona's Celanex products is about 250°C, which is 27°C above the nominal melting temperature we measured for PBT using DSC.<sup>21</sup> Taking these facts into account, it was decided to normalize the MFIs of the polyesters using temperatures that corresponded to a constant  $\Delta T$ , where  $\Delta T = T_s - T_m$  and  $T_s$  is the rheometer set temperature and  $T_m$  is the polymer melting temperature. Thus, the MFI of the virgin PBT, PPT, and PET polymers were determined at 250, 255, and 285°C, respectively. The target MFI was 20, which is representative of PBT used in commercially available injection-moldable materials. As shown in Table I, the MFIs of the virgin polyesters used for the study were quite similar at a constant  $\Delta T$  of 27°C.

### Determination of Equilibrium Melting Temperatures

Crystallization is a process of phase transformation and thus can be described in terms of the Gibbs free-energy equation:

$$\Delta G = (H_{\text{crystal}} - H_{\text{melt}}) - T(S_{\text{crystal}} - S_{\text{melt}}) = \Delta H - T\Delta S \quad (1)$$

The thermodynamic driving force for the transformation is the lowering of the temperature below the equilibrium melting temperature, defined as  $T_m^o = \Delta H/\Delta S$ , such that  $\Delta G$  is negative. As a result, a comparison of the inherent crystallizability of polymers of different chemical composition must be done at equivalent supercooling  $\Delta T$ , where  $\Delta T = T_m^o - T_c$  and  $T_c$  is the crystallization temperature. A similar approach to comparing the crystallization rate of a homopolymer and its copolymers was used by Hybart and Pepper.<sup>22</sup>

$T_m^o$  for the polyesters under investigation was determined in the usual way using the Hoffman-Weeks equation<sup>23</sup>:

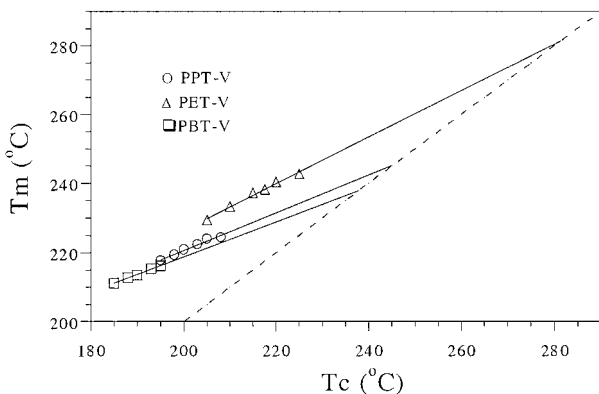


**Figure 1** Hoffman-Weeks plots for the determination of equilibrium melting temperatures for PBT, PPT, and PET.

$$T_m = T_m^\circ(1 - 1/\gamma) + T_c/\gamma \quad (2)$$

where  $T_m$  is the experimental melting temperature and  $\gamma$  is a factor that depends on the final lamellar thickness. This equation was developed on the premise that, at low levels of crystallinity, the thickness of a growing crystal is proportional to the thickness of the nucleus that initiated crystal growth. Since nucleation theory predicts that the thickness of a stable nucleus varies with  $1/\Delta T$ ,  $T_m$  will vary with  $T_c$ .<sup>23</sup> Using eq. (2),  $T_m^\circ$  can be determined by plotting  $T_m$  as a function of  $T_c$  and extrapolating the plot to the  $T_m = T_c$  line. This procedure is equivalent to an extrapolation to infinite lamellar thickness. As pointed out by Alamo and coworkers<sup>19</sup> the range of  $T_c$ s used for the plot must be controlled to minimize crystal thickening such that  $\gamma$  remains constant over the entire range of  $T_c$ s. These investigators found that the use of relatively high  $T_c$ s was problematic due to the higher rate of crystal thickening.

For both PBT and PPT, two melting endotherms were observed on heating isothermally crystallized samples. Double melting peaks for PBT have been reported by several investigators<sup>14,24</sup> and can be attributed to the existence of a melting and recrystallization process, in which crystals grown at  $T_c$  partially melt and recrystallize during the heating run to produce a higher-temperature melting endotherm associated with the newly formed, thicker crystals. Since the lower-temperature endotherm represents melting of the crystals grown at  $T_c$ , this endotherm was used for the determination of  $T_m^\circ$  for both PBT and PPT. For PET, similar melting behavior to PBT and PPT was observed, with the exception

that the low-temperature endotherm associated with crystals grown at  $T_c$  exhibited some overlap with the high-temperature endotherm associated with the crystals produced by the recrystallization process; however, the peak of the low-temperature melting endotherm was discernible, allowing for  $T_m^\circ$  to be determined.

Figure 1 shows the  $T_m$  versus  $T_c$  plot used to determine  $T_m^\circ$  for the polyesters under investigation.  $T_m$  varied linearly with  $T_c$  for all three polymers, with the slopes of the lines ranging from 0.50 for PBT to 0.67 for PET. These results suggested that artifacts in the extrapolation caused by secondary crystallization were avoided and the values of 238, 245, and 281°C for the  $T_m^\circ$  of PBT, PPT, and PET, respectively, were accurate. A  $T_m^\circ$  of 238°C for PBT is similar to the value obtained by Runt and coworkers<sup>25</sup> (236°C), Marrs and coworkers<sup>26</sup> (236°C), and Pracella and coworkers<sup>16</sup> (242°C), whereas a  $T_m^\circ$  of 281°C for PET is similar to that obtained by Barrett and associates<sup>27</sup> (285°C) and Reinsch and associates<sup>28</sup> (277°C). To our knowledge, no previous reports of  $T_m^\circ$  for PPT exist.

#### Overall Rate of Crystallization for Virgin Polyesters

Figure 2 shows representative crystallization isotherms for the virgin polymers, where  $X(t)$  is the ratio of the amount of polymer crystallized at time  $t$  to the total amount of polymer crystallized; and  $t = t_{\text{step}} - t_{\text{start}}$ , where  $t_{\text{step}}$  is the time elapsed from obtaining temperature control at  $T_c$  and  $t_{\text{start}}$ , the time required for the onset of crystallization to be observed. From these isotherms, the half-time of crystallization ( $t_{1/2}$ ), defined as the time required for  $X(t) = 0.5$ , was determined.

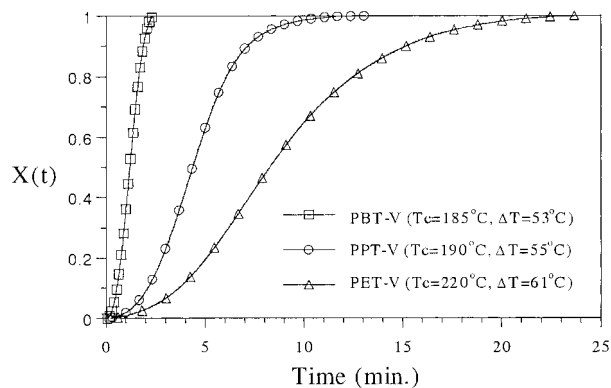


**Figure 2** Representative crystallization isotherms for virgin PBT, PPT, and PET.

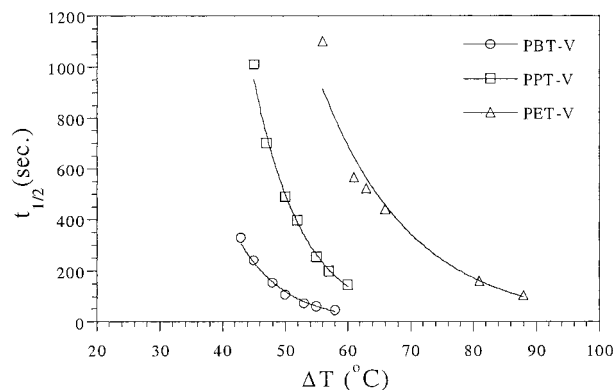


**Figure 3** Plots of  $t_{1/2}$  versus  $\Delta T$  for virgin PBT, PPT, and PET.

Typically,  $t_{1/2}$  or  $1/t_{1/2}$  is taken as a measure of the overall rate of crystallization of a polymer. Figure 3 shows how  $t_{1/2}$  varied with supercooling for the virgin polymers. From this figure, it can be seen that  $t_{1/2}$  decreased or crystallization rate increased with increasing supercooling, as expected, since crystallization is nucleation controlled over this temperature range.<sup>29</sup> Higher supercoolings, in which crystallization would be under diffusion control, were not investigated, since PBT cannot be adequately quenched to a completely amorphous state. Furthermore, crystallization during commercial processing techniques such as injection molding occurs from the melt and, thus, is of greater interest for this study. A comparison of  $t_{1/2}$  values at equivalent supercooling clearly showed that the rate of crystallization for the three polymers followed the trend: PBT > PPT > PET. To further illustrate and quantify the difference in crystallization rate between PPT and the other two polyesters over the range of crystallization temperatures investigated, the exponential fit of the  $t_{1/2}$  data shown in Figure 3 was used to generate a plot of the relative rates of crystallization for PPT and PBT as well as PPT and PET. As shown in Figure 4, the overall rate of crystallization  $k$ , defined in the traditional manner as  $k = 1/t_{1/2}$ , which allows the rate to be expressed in units of  $s^{-1}$ , for PPT ( $k_{\text{PPT}}$ ) was about fourfold lower than that of PBT over the entire temperature range investigated and about 3.5–5.0 fold faster than PET.

In addition to providing overall rates of crystallization, the crystallization isotherms were used to obtain some insight into the mechanism of crystallization by analyzing the data in the form of the Avrami equation:

$$X(t) = 1 - \exp(-k_A/t^n) \quad (3)$$

where  $k_A$  is the kinetic constant and  $n$  is the Avrami exponent describing the crystal growth geometry and nucleation mechanism.<sup>30</sup> The constant  $k_A$  is related to  $t_{1/2}$  and thus  $k$ , through the following relationship:

$$t_{1/2} = 1/k = [(\ln 2)/k_A]^{1/n} \quad (4)$$

The Avrami parameters can be determined by plotting the data according to a rearranged version of eq. (3):

$$\ln\{-\ln[1 - X(t)]\} = n \ln t + \ln k_A \quad (5)$$

where a plot of  $\ln\{-\ln[1 - X(t)]\}$  versus  $\ln t$  yields a straight line with a slope equal to  $n$  and an intercept equal to  $\ln k_A$ . Representative Avrami plots for the virgin polymers are shown in Figure 5. Linearity was obtained up to about  $X(t) = 0.9, 0.8,$  and  $0.6$  for PBT, PPT, and PET, respectively. Considering the crystallization isotherms shown in Figure 2, these values of  $X(t)$  appear to correspond to a change in the mechanism of crystallization from primary crystallization to secondary crystallization. The Avrami equation was based on the assumption that the radial growth of crystals occurs at a constant velocity and, thus, impingement of crystals with one another does not occur. As a result, the portion of the crystallization isotherms associated only with primary crystallization (crystallization before impingement) was used to determine the Avrami constants.<sup>30</sup>

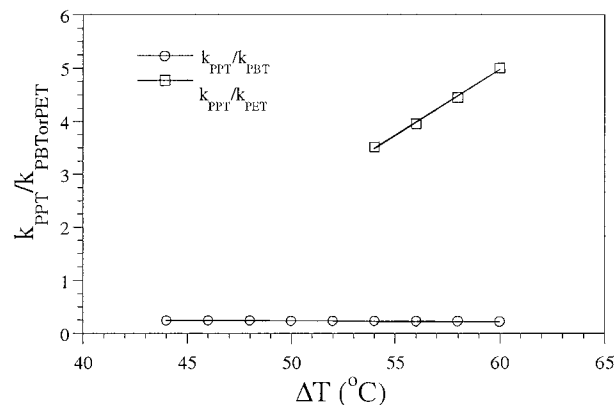


**Figure 4** Ratio of the overall crystallization rate for PPT-V relative to PBT-V and PPT-V relative to PET-V as a function of supercooling.

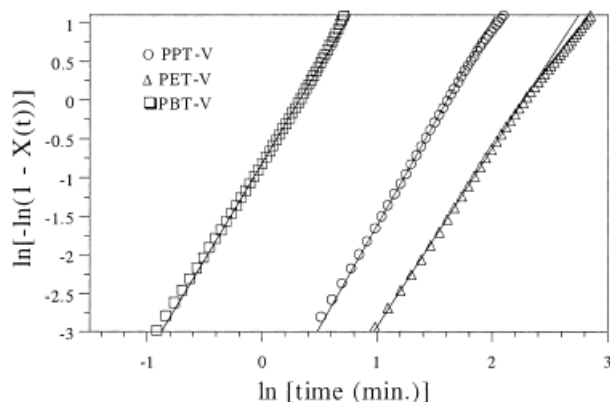


**Figure 5** Representative Avrami plots for virgin PBT ( $T_c = 185^\circ\text{C}$ ,  $\Delta T = 53^\circ\text{C}$ ), PPT ( $T_c = 190^\circ\text{C}$ ,  $\Delta T = 55^\circ\text{C}$ ), and PET ( $T_c = 220^\circ\text{C}$ ,  $\Delta T = 61^\circ\text{C}$ ).

Tables II, III, and IV list the Avrami exponents obtained for the virgin polymers as a function of supercooling. The average of the Avrami exponents for virgin PBT, PPT, and PET was 2.48, 2.54, and 2.30, respectively. The average Avrami

exponent determined for PBT and PET appears to be in good agreement with values reported by other investigators. For example, Gilbert and Hybart<sup>15</sup> reported  $n_{\text{avg}} = 2.6$ ; Pratt and Hobbs,<sup>13</sup>  $n_{\text{avg}} = 2.8$ ; Pracella and coworkers<sup>16</sup>  $n_{\text{avg}} = 2.75$ ; and Marrs and coworkers<sup>26</sup> reported Avrami exponents that ranged between 2.0 and 2.5 for PBT. For PET, Xanthos and coworkers<sup>31</sup> reported  $n_{\text{avg}} = 2.35$  and Kim and Kim,<sup>32</sup>  $n_{\text{avg}} = 2.37$ .

The similarity of the average Avrami exponent obtained for PPT to that for PBT and PET suggests that the crystallization mechanism of PPT is similar to PBT and PET. The only report known to describe an Avrami exponent for PPT was that by Bulkin and associates,<sup>17</sup> in which they report  $n = 1.62$  at  $65^\circ\text{C}$ . The discrepancy between  $n$  determined by these authors and  $n_{\text{avg}}$  reported in this study is most likely due to a difference in the nature of the rate-determining step of crystallization. At  $65^\circ\text{C}$  (the crystallization temperature used by Bulkin and coworkers<sup>17</sup>), the crystallization rate is limited by diffusion of molecules at the

**Table II** Avrami Kinetic Constants ( $k_A$ ) and Exponents ( $n$ ) for PBT-Based Materials

Sample <sup>a</sup>	$\Delta T$ ( $^\circ\text{C}$ )	$T_c$ ( $^\circ\text{C}$ )	$n$	$k_A$ ( $\text{s}^{-n}$ )	$r^2$
PBT-V	58	180	2.47	$5.61 \times 10^{-5}$	0.99962
PBT-V	55	183	2.50	$2.46 \times 10^{-5}$	0.99966
PBT-V	53	185	2.49	$1.65 \times 10^{-5}$	0.99989
PBT-V	50	188	2.43	$9.00 \times 10^{-6}$	0.99917
PBT-V	48	190	2.48	$2.74 \times 10^{-6}$	0.99917
PBT-V	45	193	2.43	$1.18 \times 10^{-6}$	0.99864
PBT-V	43	195	2.55	$2.79 \times 10^{-7}$	0.99872
PBT-M	43	195	2.56	$1.47 \times 10^{-4}$	0.99995
PBT-M	38	200	2.66	$6.37 \times 10^{-6}$	0.99986
PBT-M	36	202	2.73	$1.40 \times 10^{-6}$	0.99975
PBT-M	34	204	2.80	$2.26 \times 10^{-7}$	0.99983
PBT-M	33	205	2.96	$3.58 \times 10^{-8}$	0.99997
PBT-T	38	200	2.68	$6.14 \times 10^{-4}$	0.99989
PBT-T	33	205	2.61	$2.31 \times 10^{-5}$	0.99976
PBT-T	30	208	2.56	$2.58 \times 10^{-6}$	0.99912
PBT-T	29	209	2.61	$8.21 \times 10^{-7}$	0.99957
PBT-T	28	210	2.60	$3.10 \times 10^{-7}$	0.99923
PBT-S	38	200	2.79	$2.99 \times 10^{-5}$	0.99717
PBT-S	35	203	3.30	$5.37 \times 10^{-7}$	0.99866
PBT-S	33	205	3.18	$2.18 \times 10^{-7}$	0.99885
PBT-S	31	207	3.91	$2.62 \times 10^{-10}$	0.99593
PBT-S	29	209	4.55	$5.03 \times 10^{-13}$	0.99878

<sup>a</sup> V and M indicate virgin and melt-mixed samples, respectively; T and S indicate the presence of 0.50 pph talc and sodium stearate, respectively.

**Table III Avrami Kinetic Constants ( $k_A$ ) and Exponents ( $n$ ) for PPT-Based Materials**

Sample <sup>a</sup>	$\Delta T$ (°C)	$T_c$ (°C)	$n$	$k_A$ (s <sup>-n</sup> )	$r^2$
PPT-V	60	185	2.61	$1.52 \times 10^{-6}$	1.00000
PPT-V	57	188	2.57	$8.51 \times 10^{-7}$	0.99998
PPT-V	55	190	2.59	$4.03 \times 10^{-7}$	0.99995
PPT-V	52	193	2.45	$2.96 \times 10^{-7}$	0.99996
PPT-V	50	195	2.61	$6.51 \times 10^{-8}$	0.99997
PPT-V	47	198	2.45	$7.32 \times 10^{-8}$	0.99991
PPT-V	45	200	2.48	$2.42 \times 10^{-8}$	0.99992
PPT-M	50	195	2.52	$1.63 \times 10^{-6}$	0.99997
PPT-M	47	198	2.66	$2.41 \times 10^{-7}$	0.99988
PPT-M	45	200	2.64	$1.44 \times 10^{-7}$	0.99997
PPT-M	42	203	2.75	$2.91 \times 10^{-8}$	0.99998
PPT-M	40	205	2.97	$2.80 \times 10^{-9}$	0.99999
PPT-T	50	195	2.35	$6.64 \times 10^{-6}$	0.99988
PPT-T	46	199	2.51	$6.49 \times 10^{-7}$	0.99996
PPT-T	42	203	2.89	$2.19 \times 10^{-8}$	0.99997
PPT-T	40	205	3.04	$2.34 \times 10^{-9}$	0.99995
PPT-S	50	195	2.60	$3.60 \times 10^{-6}$	0.99999
PPT-S	45	200	2.81	$5.35 \times 10^{-7}$	0.99994
PPT-S	42	203	3.11	$1.73 \times 10^{-8}$	0.99949
PPT-S	40	205	3.34	$7.78 \times 10^{-10}$	0.99950

<sup>a</sup> V and M indicate virgin and melt-mixed samples, respectively; T and S indicate the presence of 0.50 pph talc and sodium stearate, respectively.

crystal growth front (diffusion control), whereas at temperatures closer to the melt temperature, as used in this study, the rate-limiting step of the crystallization process is the nucleation rate (nucleation control). According to Avrami theory, as discussed by Hiemenz,<sup>30</sup> a switch of the rate-determining step from diffusion control to nucleation control for three-dimensional spherulitic growth resulting from instantaneous nucleation increases the Avrami exponent from 1.5 to 3.

#### Effect of Melt-Mixing on Overall Crystallization Rate

Figures 6, 7, and 8 show the effect of melt-mixing and the presence of talc and sodium stearate on the crystallization rate of PBT, PPT, and PET, respectively. Interestingly, the process of melt-mixing resulted in a dramatic increase in crystallization rate for all three polyesters. The increase in crystallization rate induced by the melt-mixing process may stem from one or a combination of the following factors: (1) a decrease in molecular weight resulting from degradation; (2) an increase in nucleation density resulting from the

introduction of adventitious impurities; (3) a decrease in entanglement density; or (4) an increase in nucleation density resulting from an increase in the order or alignment of polymer chains in the melt. With regard to a molecular weight effect, a reduction in molecular weight can result in an increase in crystallization rate, since the mobility of polymer chains will be enhanced.<sup>10</sup> According to the molecular weight data shown in Table I, the process of melt-mixing did not significantly reduce the molecular weight of the polyesters. Melt-mixing reduced  $M_w$  by only 5.7, 9.5, and 10.8%, for PBT, PPT, and PET, respectively. As a result, it did not seem likely that the enhancement in crystallization rate obtained from the melt-mixing process was solely the result of a reduction in molecular weight. To be sure, the crystallization rate of virgin PBT, PPT, and PET polymers with molecular weights significantly lower than PBT-M, PPT-M, and PET-M samples, respectively, was measured. As shown in Table V, all of the lower molecular weight virgin samples crystallized more slowly than the higher molecular weight melt-mixed samples, confirming that the enhancement in crystallization rate caused by

**Table IV Avrami Kinetic Constants ( $k_A$ ) and Exponents ( $n$ ) for PET-Based Materials**

Sample <sup>a</sup>	$\Delta T$ (°C)	$T_c$ (°C)	$n$	$k_A$ (s <sup>-n</sup> )	$r^2$
PET-V	88	193	2.28	$1.84 \times 10^{-5}$	0.99994
PET-V	81	200	2.30	$6.14 \times 10^{-6}$	0.99984
PET-V	66	215	2.17	$1.38 \times 10^{-6}$	0.99940
PET-V	63	218	2.34	$3.09 \times 10^{-7}$	0.99996
PET-V	61	220	2.37	$2.20 \times 10^{-7}$	0.99974
PET-V	56	225	2.38	$4.01 \times 10^{-8}$	0.99954
PET-M	71	210	2.45	$1.31 \times 10^{-5}$	0.99988
PET-M	61	220	3.12	$1.71 \times 10^{-8}$	0.99920
PET-M	56	225	3.45	$4.50 \times 10^{-10}$	0.99983
PET-M	51	230	3.08	$3.33 \times 10^{-10}$	0.99974
PET-T	61	220	2.27	$4.78 \times 10^{-5}$	0.99985
PET-T	56	225	2.86	$3.27 \times 10^{-7}$	0.99975
PET-T	54	227	3.45	$5.53 \times 10^{-9}$	0.99988
PET-T	51	230	3.29	$1.55 \times 10^{-9}$	0.99911
PET-T	46	235	2.95	$8.82 \times 10^{-10}$	0.99982
PET-S	61	220	2.68	$1.18 \times 10^{-5}$	0.99576
PET-S	56	225	2.86	$1.18 \times 10^{-6}$	0.99893
PET-S	54	227	3.07	$2.00 \times 10^{-7}$	0.99938
PET-S	51	230	4.50	$5.58 \times 10^{-12}$	0.99926
PET-S	49	232	4.60	$5.07 \times 10^{-13}$	0.99814

<sup>a</sup> V and M indicate virgin and melt-mixed samples, respectively; T and S indicate the presence of 0.50 pph talc and sodium stearate, respectively.

melt-mixing was not solely the result of a decrease in molecular weight.

An increase in crystallization rate afforded by a process involving shear forces has been reported by several authors.<sup>33-38</sup> For example, Kim and Kim<sup>33</sup> explained an increase in the crystallization

rate of PET with increasing shear rate as resulting from polymer chain disentanglement caused by the shear treatment. Decreasing the entanglement density of the polymer was believed to increase nucleation rate and crystal growth rate, since the mobility of the polymer chains would be

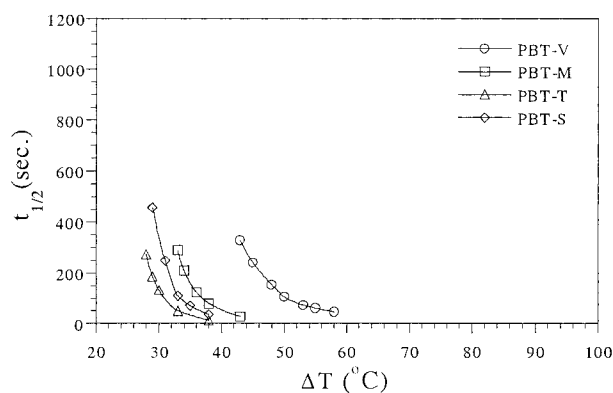


**Figure 6** Crystallization half-time ( $t_{1/2}$ ) as a function of supercooling ( $\Delta T$ ) for virgin, melt-mixed, talc-nucleated, and sodium stearate-nucleated samples of PBT.

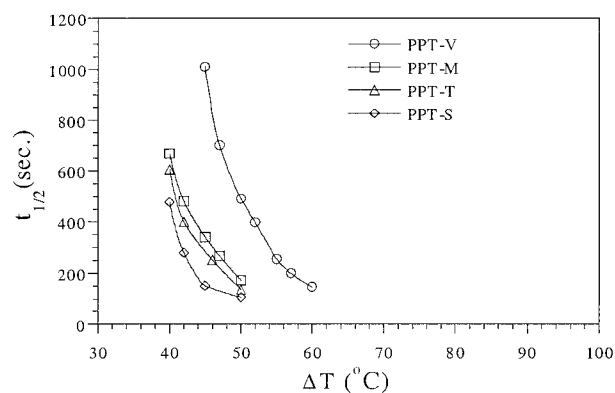


**Figure 7** Crystallization half-time ( $t_{1/2}$ ) as a function of supercooling ( $\Delta T$ ) for virgin, melt-mixed, talc-nucleated, and sodium stearate-nucleated samples of PPT.



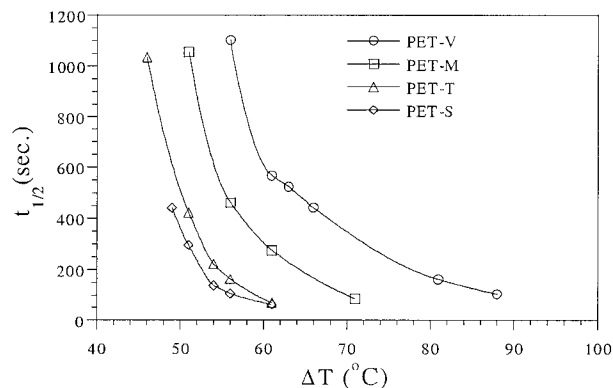


**Figure 8** Crystallization half-time ( $t_{1/2}$ ) as a function of supercooling ( $\Delta T$ ) for virgin, melt-mixed, talc-nucleated, and sodium stearate-nucleated samples of PET.

enhanced. Precedence for a decrease in entanglement density of a polymer sample by subjecting it to a shear history was provided by the rheological studies of Schreiber and associates.<sup>39-41</sup>

Khanna and coworkers<sup>35-38</sup> showed that, in addition to PET, a variety of polyamides exhibit an increase in crystallization rate when given a shear history, whereas the crystallization rate of polyethylene was unaffected by shear. The level of crystallization rate enhancement appeared to be related to the polarity of the polymer, with the more polar polymers exhibiting the greatest increase in crystallization rate.<sup>42</sup> These authors proposed that the enhancement in crystallization rate created by shear was the result of local orientation of polymer chains in the melt that, because of strong intermolecular interactions such as hydrogen bonding, is essentially permanently preserved. These regions of local order serve as nucleation centers, resulting in an enhancement in overall crystallization rate. Similar conclusions were made by Sherwood and coworkers<sup>34</sup> for polyethylene oxide and polycaprolactone. Although the increase in crystallization rate observed for

the melt-mixed polyesters under investigation was consistent with results obtained by other investigators, identification of the root cause of this rate enhancement could not be unequivocally deduced from the crystallization rate data obtained. Further work is required to fully explain the effect of melt-mixing on crystallization rate.

A comparison of the Avrami exponents obtained for the virgin polyesters and their melt-mixed analogs (Tables II-IV) shows that melt-mixing resulted in an increase in the average Avrami exponent from 2.48 to 2.74 for PBT, from 2.54 to 2.71 for PPT, and from 2.30 to 3.03 for PET. An increase in the Avrami exponent induced by shear has been previously reported by several investigators. Sherwood and coinvestigators<sup>34</sup> as well as Fritzsche and Price<sup>43</sup> showed that for polyethylene oxide crystallized under shear,  $n$  increased dramatically with shear rate. For example,  $n$  increased from a value of 3 for a quiescent melt to a value greater than 5 at high shear rate.<sup>34</sup> The results obtained by Kim and Kim,<sup>33</sup> and Khanna and associates,<sup>37</sup> which, analogous to the experiments described in our study, involve the determination of Avrami exponents for the quiescent crystallization of samples previously given a shear history showed a more modest increase in  $n$  with shear rate. For example, extrusion of a sample of virgin nylon 6 increased  $n$  from 2 to 3.<sup>37</sup> For the materials under investigation, assuming that the shear history did not affect the geometry of crystal growth, the modest increase in  $n$  produced by melt-mixing may have been the result of a shift in the mechanism of nucleation toward more sporadic nucleation, such that nuclei generation possessed a greater time dependence.<sup>44</sup>

#### Effect of Nucleating Agents on Overall Crystallization Rate

Nucleating agents are commonly used commercially to enhance the crystallization rate of semi-

**Table V** Comparison of the Overall Crystallization Rates of Melt-Mixed Materials to Lower Molecular Weight Virgin Polymers

Polymer	Description	$M_n$	$M_w$	$T_c$ (°C)	$t_{1/2}$ (s)
PBT	Virgin	20,300	49,400	202	552
PBT	Melt-mixed	33,000	73,000	202	123
PPT	Virgin	25,000	54,300	200	489
PPT	Melt-mixed	33,900	70,900	200	340
PET	Virgin	21,000	46,900	220	485
PET	Melt-mixed	29,300	61,000	220	275

crystalline polyesters. For PBT and PET, nucleating agents such as talc<sup>45</sup> or sodium stearate<sup>46</sup> have been successfully employed. Nonreactive, nonmelting nucleants such as talc have been termed *heterogeneous* nucleants, whereas reactive, soluble nucleants such as sodium stearate have been termed *chemical* nucleants. Nucleation by heterogeneous nucleants stems from molecular interactions between the polymer and the surface of the nucleant, resulting in a reduction in the free energy needed to form a stable nucleus. Chemical nucleation of condensation polymers such as PET was described by Legras and associates<sup>47,48</sup> as occurring by the reaction of alkali metal salts of organic acids with the polymer to produce chains with ionic end groups. Because of strong electrostatic interactions, these ionic end groups form clusters that reduce the local mobility of the chain, thereby facilitating the formation of stable nuclei.

As shown in Figures 6–8, both talc and sodium stearate were effective nucleants for all three polyesters. For PBT, talc allowed for faster crystallization, on a per-weight-of-nucleant basis, than sodium stearate, whereas sodium stearate was found to be more effective for PPT and PET. The molecular weight data displayed in Table I show that melt-mixing sodium stearate into the polyesters resulted in a 10.5, 20.5, and 22.5% decrease in  $M_w$  for PBT, PPT, and PET, respectively. Thus, the greater effectiveness of sodium stearate as a nucleant for PPT and PET compared to PBT may be the result of a greater extent of reaction of sodium stearate with the former. Assuming the rate constant associated with the reaction of sodium stearate with a polymer backbone ester group is similar for all three polyesters, it would be expected that the extent of reaction follow the order PET > PPT > PBT, since the concentration of ester groups increases in analogous fashion and, more important, the temperature of melt-mixing varied in the same manner.

Although compounding talc or sodium stearate into PPT and PET greatly enhanced crystallization rate, these nucleated materials still did not crystallize as fast as un-nucleated, melt-mixed PBT (PBT-M). Figure 9, which was generated by fitting  $t_{1/2}$  versus time data with an exponential fit and then calculating the ratio of rate constants for PBT-M and PPT-S, shows that the crystallization rate for PBT-M was about seven- to 12-fold higher than that obtained for PPT-S over the range of supercoolings investigated. The data ob-

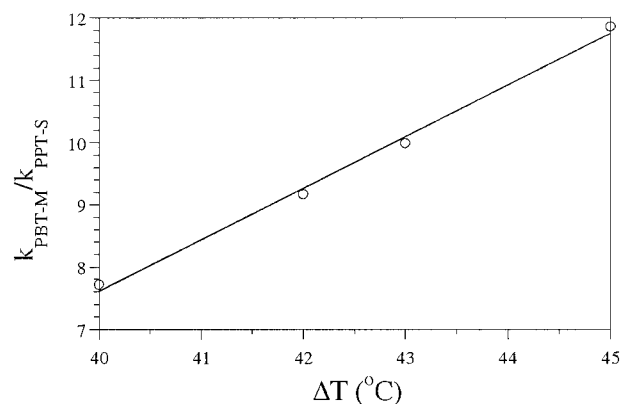


**Figure 9** Ratio of the overall crystallization rate of melt-mixed PBT (PBT-M) to sodium stearate-nucleated PPT (PPT-S) as a function of supercooling.

tained suggested that, even with the addition of nucleating agents, injection-molded materials based on PPT would not possess the same level of performance in terms of cycle time as PBT materials compounded in the absence of a nucleating agent. Previous work, which involved an investigation of the effect of talc and sodium stearate on the mechanical and viscoelastic properties of glass-filled PPT and analogous PBT materials, provides support for this conclusion.<sup>7</sup>

Comparison of the Avrami exponents generated for the samples compounded with the nucleants to the samples compounded in the absence of the nucleants (Tables II–IV) showed that Avrami exponents were essentially unchanged by nucleation with talc, whereas nucleation with sodium stearate resulted in a substantial increase in the Avrami exponents of all three polyesters. Furthermore, the Avrami exponent for sodium stearate-nucleated materials was clearly a function of crystallization temperature, with  $n$  increasing with increasing  $T_c$ .

Several reports exist that describe the Avrami exponents of PET compounded with various nucleating agents.<sup>28,46,49</sup> Przygocki and Wlochowicz<sup>49</sup> determined Avrami exponents for PET containing a variety of heterogeneous nucleating agents and found very little difference in the Avrami exponent of the nucleated materials relative to the un-nucleated virgin PET sample when the level of nucleant was 1.0 wt % or less. The Avrami exponents were between 3.0 and 4.0, and observations made using polarized light microscopy showed that nucleation was essentially instantaneous. Garcia<sup>46</sup> investigated the nucleation of PET by various metal salts including sodium

stearate. Unfortunately, Avrami exponents for sodium stearate-nucleated samples were not reported; however, Avrami exponents were reported for sodium benzoate-nucleated materials. Similar to sodium stearate, sodium benzoate can be considered a chemical nucleant since a decrease in molecular weight was observed on compounding and analysis of the polymer confirmed that sodium ions were attached. Avrami exponents obtained for sodium benzoate-nucleated PET showed a substantial increase in  $n$  with increasing crystallization temperature, which parallels the results discussed in this report for sodium stearate-nucleated PET. Garcia<sup>46</sup> found that the Avrami exponent increased from 2.31 at a crystallization temperature of 235°C to 3.74 at a crystallization temperature of 242°C for PET nucleated with 0.70 wt % sodium benzoate. No explanation was given for this variation in Avrami exponent with crystallization temperature. Reinsch and Rebenfeld<sup>28</sup> also reported an increase in Avrami exponent with increasing crystallization temperature for a commercially available PET containing a nucleating agent. Unfortunately, the composition of the nucleant was not reported.

According to Avrami theory, a change in the Avrami exponent with crystallization temperature may result from a change in crystal growth geometry and/or a change in nucleation mechanism with crystallization temperature. Assuming no change in the geometry of crystal growth, an increase in the Avrami exponent with increasing crystallization temperature suggests a change in mechanism of nucleation toward more sporadic nucleation with increasing temperature. Since changes in crystallization temperature have been shown to affect crystallite morphology,<sup>50</sup> the assumption of a constant crystallite morphology with crystallization temperature may not be valid. As a result, an explanation of the effect of crystallization temperature on the crystallization process of the sodium stearate-nucleated materials based on changes in the Avrami exponent alone is not possible. Further work, such as morphological characterization of the materials, is required for an adequate explanation of this behavior.

## CONCLUSIONS

At equivalent MFI and degree of supercooling, the crystallization rate of virgin samples of the three commercially important polyalkylene terephthal-

ates followed the trend: PBT > PPT > PET. The crystallization rate of all three virgin polyesters was found to be significantly increased by melt-mixing. This increase in crystallization rate could not be attributed solely to a molecular weight decrease resulting from the mixing process, but was believed rather to be the result of an increase in the nucleation density caused by shear forces. The exact mechanism of the crystallization rate enhancement could not be deduced from the data obtained, but previous work by others supports the contention that shear forces and their effect on entanglement density and/or polymer chain alignment were the primary factors responsible for this behavior.

The addition of 0.50 pph talc or sodium stearate as a nucleating agent increased the crystallization rate of all three polyesters. Although the addition of talc or sodium stearate into PPT and PET greatly enhanced crystallization rate, these nucleated materials still did not crystallize as fast as unnucleated, melt-mixed PBT. This result suggests that the addition of a nucleating agent alone will not allow for the production of PPT- or PET-based injection-molding materials with the same level of cycle-time performance as similar, unnucleated PBT-based materials.

Analysis of the crystallization kinetics data using the Avrami equation suggested that crystallization of all three virgin polyesters was similar and consistent with a crystallization process occurring by heterogeneous nucleation and three-dimensional spherulitic growth. Melt-mixing the virgin polyesters resulted in an increase in the Avrami exponent. Assuming no change in the geometry of crystal growth, this result indicated melt-mixing produced a change in the nucleation mechanism toward more sporadic nucleation, in which nuclei generation had a greater time dependence.

A comparison of the Avrami exponents generated for the samples compounded with the nucleating agents to the samples compounded in the absence of the nucleants showed that Avrami exponents were essentially unchanged by nucleation with talc, whereas nucleation with sodium stearate resulted in a substantial increase in the Avrami exponents for all three polyesters. In addition, the samples nucleated with sodium stearate showed a clear trend between crystallization temperature and the Avrami exponent, with the Avrami exponent increasing with increasing temperature. Although an increase in the Avrami exponent with increasing crystallization temper-

ature has been observed by others for the chemical nucleation of PET, a precise explanation of this behavior cannot be provided without knowledge of the effect of crystallization temperature on crystal growth geometry, since both nucleation behavior and crystal growth geometry affect the Avrami exponent.

## REFERENCES

- Dangayach, K.; Chuah, H.; Gergen, W.; Dalton, P.; Smith, F. *Soc Plast Eng Tech Papers* 1997, 55, 2097.
- Chuah, H. H.; Werny, F.; Langleym, T. Presented at AATCC International Conference Exhibition, 1995; Paper 98.
- Brown, H. S.; Chuah, H. H. *Chem Fibers Int* 1997, 47, 72.
- Traub, H. L.; Hirt, P.; Herlinger, H. *Chem Fibers Int* 1995, 45, 110.
- Traub, H. L.; Hirt, P.; Herlinger, H. *Angew Makromol Chem* 1995, 230, 179.
- Ward, I. M.; Wilding, M. A.; Brody, H. *J Polym Sci Polym Phys Ed* 1976, 14, 263.
- Chisholm, B. J.; Fong, P. M.; Zimmer, J. G.; Hendrix, R. *J Appl Polym Sci* 1999, 74, 889.
- Jog, J. P. *J Macromol Sci Rev Macromol Chem Phys* 1995, C35, 531.
- Verhoyen, O.; Dupret, F.; Legras, R. *Polym Eng Sci* 1998, 38, 1594.
- van Antwerpen, F.; van Krevelen, D. W. *J Polym Sci* 1972, 10, 2423.
- Lin, C. C. *Polym Eng Sci* 1983, 23, 113.
- Patkar, M.; Jabarin, S. A. *J Appl Polym Sci* 1993, 47, 1749.
- Pratt, C. F.; Hobbs, S. Y. *Polymer* 1976, 17, 12.
- Righetti, M. C.; Munari, A. *Macromol Chem Phys* 1997, 198, 363.
- Gilbert, M.; Hybart, F. J. *Polymer* 1972, 13, 327.
- Pracella, M.; Chiellini, E.; Dainelli, D. *Makromol Chem* 1989, 190, 175.
- Bulkin, B. J.; Lewin, M.; Kim, J. *Macromolecules* 1987, 20, 830.
- Bulkin, B. J.; Lewin, M.; DeBlase, F. J.; Kim, J. *Polym Mater Sci Eng* 1986, 54, 397.
- Alamo, R. G.; Viers, B. D.; Mandelkern, L. *Macromolecules* 1995, 28, 3205.
- DeLaney, D. E.; Reilly, J. F. *Plast Eng* 1998, 54, 45.
- Processing Guide; GE Plastics: Mt. Vernon, IN, 1998.
- Hybart, F. J.; Pepper, B. *J Appl Polym Sci* 1969, 13, 2643.
- Hoffman, J. D.; Weeks, J. J. *Res Natl Bur Stand US* 1962, 66A, 13.
- Hobbs, S. Y.; Pratt, C. F. *Polymer* 1975, 16, 462.
- Runt, J.; Miley, D. M.; Zhang, X.; Gallagher, K. P.; McFeaters, K.; Fishburn, J. *Macromolecules* 1992, 25, 1929.
- Marrs, W.; Peters, R. H.; Still, R. H. *J Appl Polym Sci* 1979, 23, 1077.
- Barrett, L. W.; Sperling, L. H.; Gilmer, J.; Mylonakis, S. G. *J Appl Polym Sci* 1993, 48, 1035.
- Reinsch, V. E.; Rebenfeld, L. *J Appl Polym Sci* 1994, 52, 649.
- Fatou, J. G. *Encyclopedia of Polymer Science and Engineering—Supplement Volume*; Kohlmetz, E.; Levy, C.; Walter, P., Eds.; Wiley: New York, 1989; p 231.
- Hiemenz, P. C. *Polymer Chemistry*; Marcel Dekker: New York, 1984.
- Xanthos, M.; Baltzis, B. C.; Hsu, P. P. *J Appl Polym Sci* 1997, 64, 1423.
- Kim, S. P.; Kim, S. C. *Polym Eng Sci* 1991, 31, 110.
- Kim, S. P.; Kim, S. C. *Polym Eng Sci* 1993, 33, 83.
- Sherwood, C. H.; Price, F. P.; Stein, R. S. *J Polym Sci Symp* 1978, 63, 77.
- Khanna, Y. P.; Taylor, T. J. *Polym Eng Sci* 1988, 28, 1042.
- Khanna, Y. P.; Reimschuessel, A. C. *J Appl Polym Sci* 1988, 35, 2259.
- Khanna, Y. P.; Reimschuessel, A. C.; Banerjee, A.; Altman, C. *Polym Eng Sci* 1988, 28, 1600.
- Khanna, Y. P.; Kumar, R.; Reimschuessel, A. C. *Polym Eng Sci* 1988, 28, 1607.
- Schertzer, R.; Rudin, A.; Schreiber, H. P. *J Appl Polym Sci* 1986, 31, 809.
- Ajji, A.; Carreau, P. J.; Schreiber, H. P. *J Polym Sci Polym Phys Ed* 1986, 24, 1983.
- Rudin, A.; Schreiber, H. P. *Polym Eng Sci* 1983, 23, 422.
- Khanna, Y. P.; Kumar, R.; Reimschuessel, A. C. *Polym Eng Sci* 1988, 28, 1612.
- Fritzsche, A. K.; Price, F. P. *Polym Eng Sci* 1974, 14, 401.
- Long, Y.; Shanks, R. A.; Stachurski, Z. H. *Prog Polym Sci* 1995, 20, 651.
- Groeninckx, G.; Berghmans, H.; Overbergh, N.; Smets, G. *J Polym Sci Polym Phys Ed* 1974, 12, 303.
- Garcia, D. *J Polym Sci Polym Phys Ed* 1984, 22, 2063.
- Legras, R.; Mercier, J. P.; Nield, E. *Nature* 1983, 304, 432.
- Legras, R.; Bailly, C.; Daumerie, M.; Dekoninck, J. M.; Mercier, J. P.; Zichy, V.; Nield, E. *Polymer* 1984, 25, 835.
- Przygocki, W.; Wlochowicz, A. *J Appl Polym Sci* 1975, 19, 2683.
- Chatterjee, A. M.; Price, F. P.; Newman, S. *J Polym Sci Polym Phys Ed* 1975, 13, 2369.